11th International Conference on Fracture Mechanics of Concrete and Concrete Structures
FraMCoS-11
J. M. Chandra Kishen, A. Ramaswamy, S. Ray and R. Vidyasagar (Eds)
https://doi.org/10.21012/FC11.092330

RAILWAY INFRASTRUCTURE ASSET ANALYSIS USING A GLOBAL-LOCAL APPROACH

A.L. GAMINO[†], R.R. SANTOS[†], L.A.G. BITENCOURT JR.[†], T.N. BITTENCOURT[†] AND M.M. FUTAI[†]

[†] Dept. of Structural and Geotechnical Engineering
School of Engineering, University of Sao Paulo
Prof. Almeida Prado 83, 05508-070 Sao Paulo, Brazil
e-mail: gamino@alumni.usp.br, www.poli.usp.br

Keywords: Reinforced Concrete, Smeared crack model, Global-local approach, Railway infrastructure, Finite element method

Abstract: The global-local modeling methodology is used to evaluate specific regions of a structural system. A global model represents the entire system under study, while critical domains are assessed in detail by a submodeling routine employing more refined models. The advantages of this hierarchical modeling are related to reducing the need for complex transition regions in solid elements and the versatility in testing different geometries in the submodel region. Furthermore, it allows for a reduction in the computational power required to solve the problem. However, ensuring a good transfer of the boundary conditions between the different models is essential. For large and complex infrastructures, such as bridges, numerical analyses sometimes become time-consuming when more complex evaluations are required. Therefore, using simplified models to reproduce global behavior and more complex modeling strategies in critical locations can be an alternative to comply with this requirement. The present paper aims to employ a global-local approach to analyze a reinforced concrete railway bridge. Thus, the global and local models employed numerical analyses using solid tetrahedral finite elements. The local region presented a greater mesh discretization for the submodeling. Additionally, the local model allows inserting steel reinforcement details and specific constitutive laws for the materials utilized in the described region of the railway infrastructure. The obtained results enable the evaluation of the formation and propagation of cracks and the identification of damages located in the structural elements with greater precision. The methodology can improve condition assessment and support the inspection and maintenance of critical infrastructure assets.

1 INTRODUCTION

Due to the localized nature of the problem, correct crack modeling is a complex topic as it deals with discontinuity in the displacement field. In the numerical simulation of cracked concrete structures using the Finite Element Method (FEM), choosing the adequate type of model to be used in each situation is crucial. Generally, the most widespread representations can be classified as distributed or discrete [1].

Notably, two aspects are of particular importance: (i) represent the crack, (ii) simulate the behavior of the cracked material. Thus, for a realistic analysis of concrete structures, an effective modeling strategy for the different behaviors of the component materials of a structural system is essential.

In the discrete form representation, the crack is modeled by separating the elements edges. In

the Finite Element Method, discrete cracks are modeled unless the crack trajectory is known in advance, generally changing the mesh to support propagation. Additionally, there is the possibility of using interface elements with adequate constitutive laws to simulate the cohesive effect related to the cracks opening [2].

This mesh redefinition has a high computational cost, making it difficult to use these models when several cracks are scattered along the part, as in the case of reinforced concrete (RC) structures. Other possibilities refer to using nodal enrichment or finite elements [3].

In smeared crack models [4], the discontinuity of the displacement field caused by the crack is spread along the element, altering its constitutive equation. Even knowing that the assumed displacement continuity is incompatible with the actual discontinuity, models of this type have been the most used over the years because their computational application is quite simple, and they can adequately model the global structural behavior of reinforced concrete parts.

However, when combined with models based on Fracture Mechanics to simulate the behavior of cracked concrete, these models depend on the finite element mesh used in the numerical analysis [5].

The semi-empirical models are developed through values obtained in tests of reinforced concrete components. This model is based on experimental values, and they can simulate not only the various phenomena that occur during the cracking of reinforced concrete, such as concrete softening and the contribution of concrete between cracks (tension-stiffening), but also its interaction. Nonetheless, when these models are employed, it is impossible to separately analyze the influence of each of these phenomena on the global response of the structure.

Coupled with the concrete degradation model, it becomes advantageous to use submodeling techniques, starting from the discretization of regions of interest in which the degradation of the element occurs more intensely. Thus, crack propagation regions more consistent with experimental observations can be predicted [6].

Other applications of the submodeling technique refer to steel structure evaluation, predicting material plastification and fatigue behavior in connections between elements [7].

2 SMEARED CRACK APPROACH

The smeared crack model implemented in Abaqus 6.14-6 was used based on a rotational technique using four steps:

- Definition of the concrete behavior under uniaxial compression;
- Description of a failure surface based on crack growth law;
- Definition of a tension-stiffening model;
- Calibration of the shear retention factor.

The compressed concrete behavior under the uniaxial aspect must be done according to the contribution of experimental data or even from values prescribed by design codes.

The failure surface allows the detection of the beginning of the crack propagation within the plane of incidence of principal stresses (Figure 1). In this sense, several failure surfaces can be employed for supporting the incidence and propagation of discontinuities in the element domain.

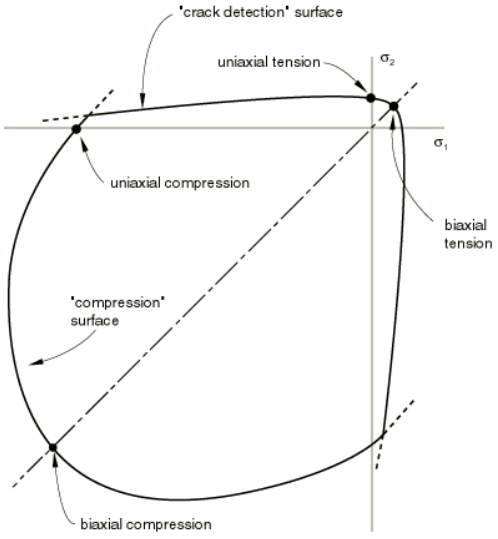

Figure 1: Failure criterion adopted for concrete [8].

Various functions can be adopted for tension-stiffening models. For the linear model

displayed in Figure 2, used in this paper, the relationships between stresses and deformations in the cracks have a direct and linear proportion, and the area below the graph represents the relationship between the fracture energy in mode I and the crack bandwidth (square root of the finite element area of concrete).

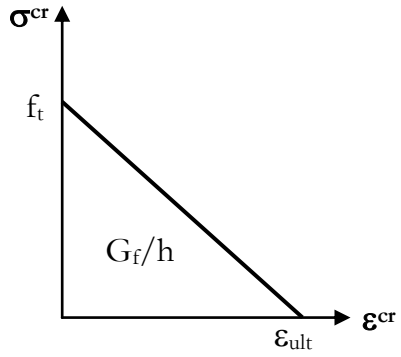

Figure 2: Tension-stiffening linear model.

In this situation, the following constitutive equations are valid:

$$\sigma^{cr}(\varepsilon^{cr})/f_t = 1 - \varepsilon^{cr}/\varepsilon^{cr}{}_u \quad (1)$$

$$w = 2G_f / f_t \quad (2)$$

$$w = \varepsilon^{cr} h^{cr} \quad (3)$$

where f_t is concrete tensile strength, G_f is the fracture energy in mode I, w is the crack width, and h^{cr} is the crack bandwidth.

Finally, the material shear retention factor (parameter β) must be adopted as an input attribute. Figure 3 illustrates how β affects the transverse stiffness of concrete.

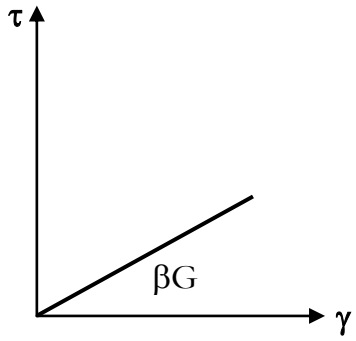

Figure 3: Effect of shear retention factor.

Thus, given the constitutive matrix of the crack above, the shear stiffness is given by:

$$D_{sec} = \beta G / (1 - \beta) \quad (4)$$

where G represents the concrete shear modulus.

The β factor can assume values between 0 and 1. For zero or near zero β values, the concrete has a minimal shear stiffness. Conversely, an infinite shear stiffness is obtained for a unitary value, which will dispense the formation of cracks in this direction.

This paper tested the ability to identify progressive damage in concrete using the smeared cracking technique in conjunction with the submodeling (solid-to-solid) approach using three-dimensional solid finite elements.

3 RC RAILWAY BRIDGE SECTION

For this paper, a section of a six-span reinforced concrete railway bridge located in the northern region of Brazil was employed as a case study. The superstructure is supported on the pile caps by neoprene bridge bearings, and the infrastructure comprises pile caps and caissons supported by a rock layer (Figure 4).

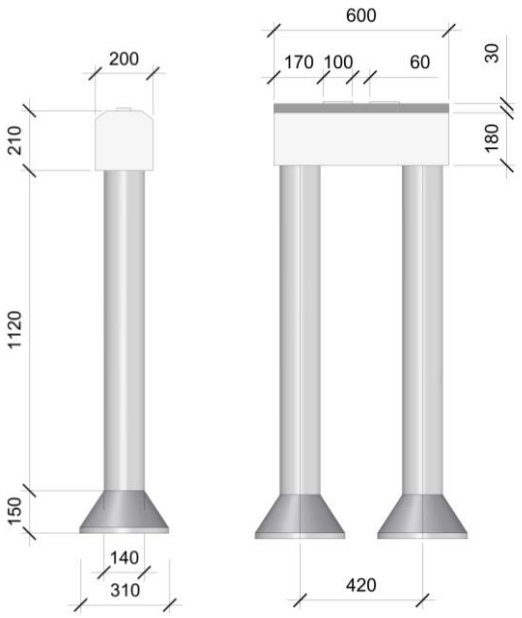

Figure 4: RC infrastructure bridge studied section (geometry developed in Rhino 7, dimensions in "cm").

3.1 Global-local strategy

The computational modeling strategy was

developed in Abaqus, version 6.14-6. The adopted cutting plan is illustrated in Figure 5 and represents the land surface in which the foundations are embedded.

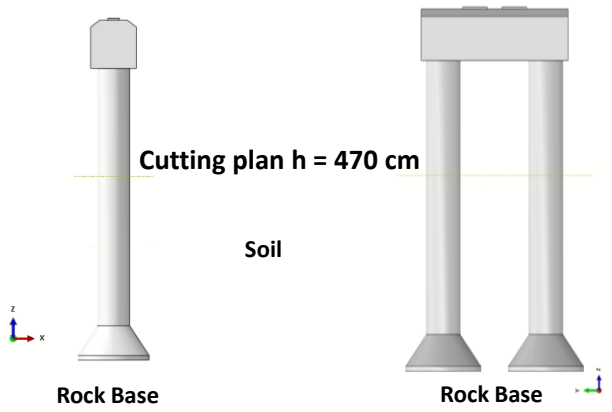

Figure 5: Cutting plan strategy to create a submodel in Abaqus.

For the finite element mesh, elements C3D10 type were used, containing ten nodes with quadratic interpolation and four Gauss integration points. An unstructured mesh was used for both local and global models. Additionally, a solid-to-solid strategy was employed at the same hierarchy level (Figure 6). An unstructured mesh was used in the local and global models. Additionally, the technique employed in Abaqus was solid-to-solid at the same hierarchy level.

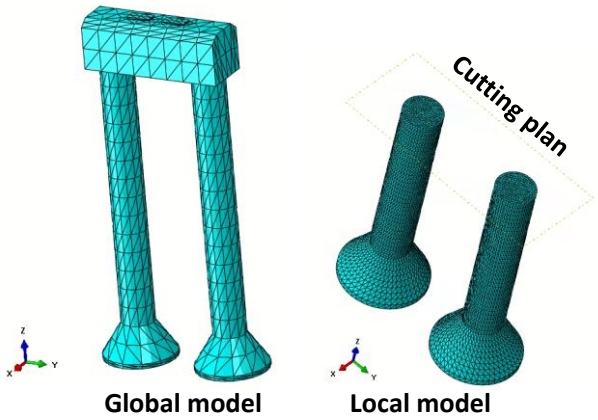

Figure 6: Global and local FE model in Abaqus.

For the main model, mesh (global) elements with 80 cm of characteristic size were used, totaling 2,932 C3D10 elements. For the local model, elements of characteristic size equal to 20 cm were employed, accounting for 39,071 C3D10 elements.

For the compressed concrete, the stress-strain ratio was adopted based on the rules of the Brazilian design code for concrete structures, NBR 6118 [9]:

$$\sigma_c = 0.85 f_c m \quad (5)$$

$$m = (1-(1-\varepsilon_c/\varepsilon_{c2})^2 \quad (6)$$

where ε_{c2} represents the concrete deformation at the beginning of the plastic behavior.

Table 1 presents the elastic parameters of the concrete adopted in the asset.

Table 1: Concrete elastic parameters used in asset and computational model.

Young's modulus	21800 MPa
Poisson's ratio	0.20
Mass density	25 kN/m³

Figure 7 illustrates the stress-strain behavior of concrete for uniaxial compressive stresses for smeared crack model applied in global-local models.

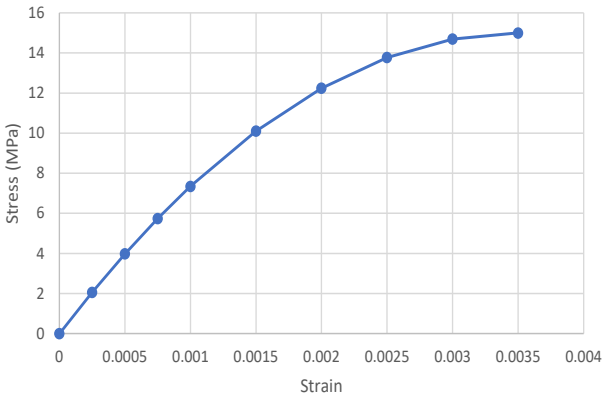

Figure 7: Stress-strain relationship for compressed concrete.

Table 2 shows the nonlinear parameters applied in computational models using the smeared crack approach. The values of the smeared crack variables were based on previous studies [10-12].

Table 2: Concrete nonlinear parameters used in the computational model for smeared crack model.

Ratio 1	21.37 MPa
Ratio 2	0.1216
Ratio 3	0.44
Ratio 4	0.33
Rho close (shear retention)	0.1
Eps max (shear retention)	0.002
Epsilon (tension stiffening, strain)	0.002

4 COMPUTATIONAL RESULTS

4.1 Load and analysis

Loads were applied on the neoprene bearing pads representing the loads in service with a value equal to 1,673 kN per pad (Figure 8).

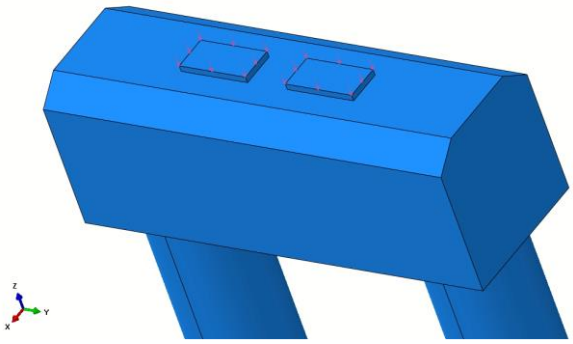

Figure 8: Load applied in neoprene pads.

Static nonlinear analysis was performed with increments of automatic loads, ranging from 1.0×10^{-5} to 2.0×10^{-2} of the proportion of total loads. The nonlinear analysis was performed based on loading control. In the modeling technique employed, the displacements originating from the global model were transmitted to the local model in the three directions (x, y, and z), using the cutting plan (Figure 6) to compose a continuity process between the models.

4.2 Computational results

In the global model, the cracks were initiated in the bottom region of the foundation block for a proportion of 0.315 of the total service loads (Figure 9). For the total load in service, the global model presented deformations in the maximum cracks below the block of the order of 4.024×10^{-4} and for the caissons of the order of 2.682×10^{-4} (Figure 10).

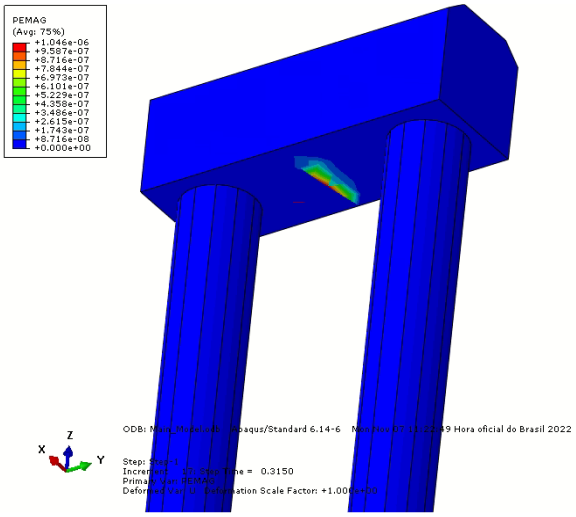

Figure 9: Formation and initial propagation of cracks in the foundation block.

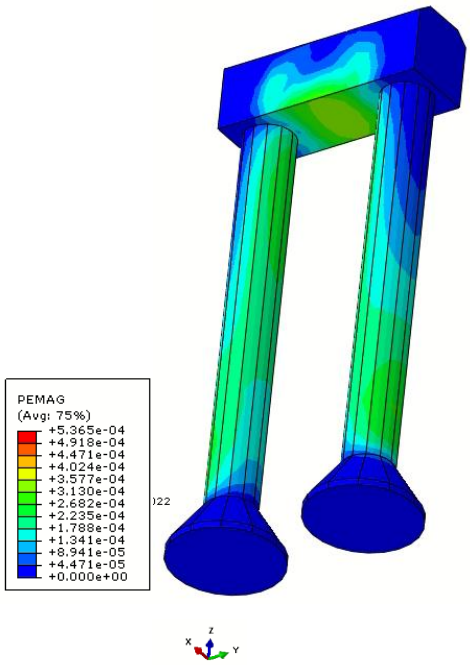

Figure 10: Final crack pattern in the global model for the full-service load.

Considering a load level of 0.515 (Figure 11), there was no formation of cracks in the caissons. This situation was later verified in the local model.

For the principal stresses in the caissons concerning the global model (Figure 12), the results displayed stresses of 0.2 MPa, and no

stress concentrations were observed in any region of the foundations.

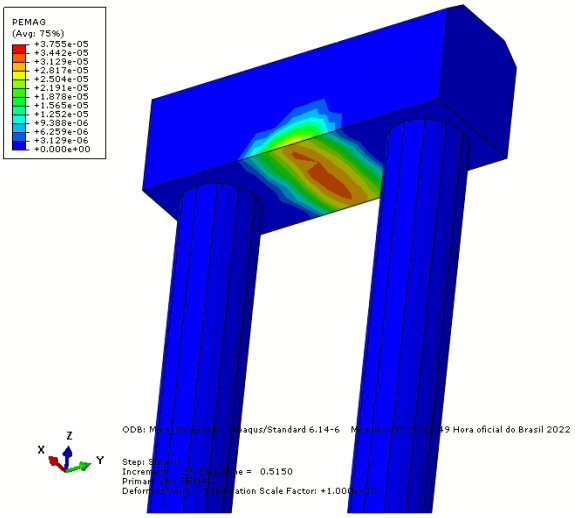

Figure 11: Crack pattern in the global model for a load level of 0.515.

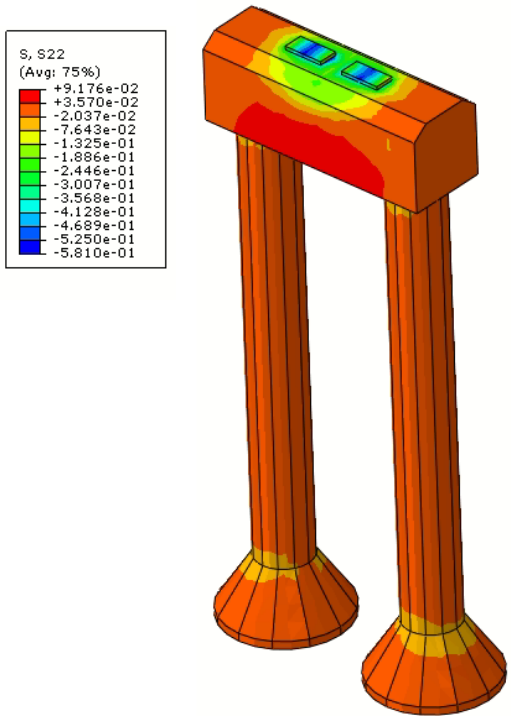

Figure 12: Principal stresses for full-service load in the global model (kN/cm²).

The results in the local model for the cracking pattern showed that the first cracks formed for a load level of about 0.395 of the service loads. As displayed in Figure 13, these cracks were concentrated in the region where the caissons present a geometry alteration.

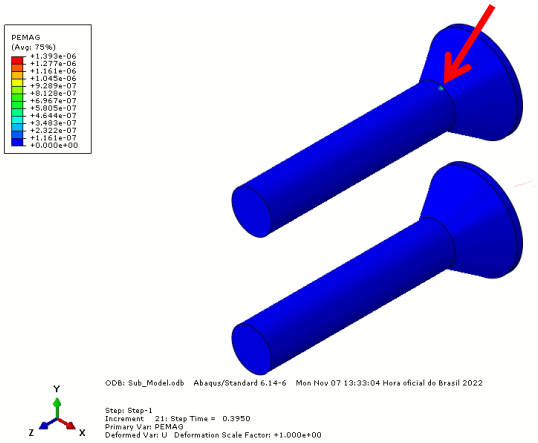

Figure 13: Initial crack growth in the local model.

By comparing the cracking patterns illustrated in Figure 11 and Figure 13, it can be noted that the global model could not adequately predict the foundations' cracking load since there were no cracks in the caissons in the global model until 0.515 of the service loads. For this load level (0.515, Figure 14), a considerable and representative region of cracks was noticed in the foundations for the local model, displaying the advantage of using this model for more accurate analyses of cracking patterns.

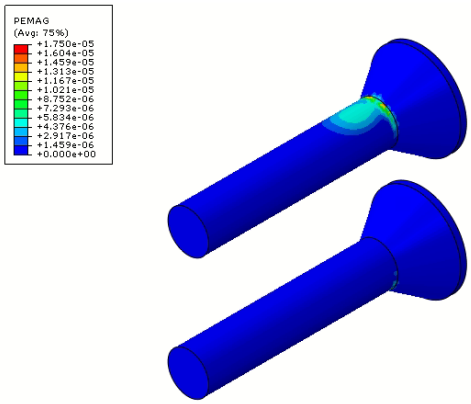

Figure 14: Crack pattern in the local model for load level 0.515.

The final cracking arrangement in the local model is shown in Figure 15. A greater spectrum of deformations can be observed compared to the global model for the same load level. The maximum deformation value for the local model was 2.922×10^{-4}, while the

maximum deformation was in the order of 2.682×10^{-4} (Figure 10) for the global model. These results demonstrate that the local model captures deformations with more significant values than the global model. Furthermore, the analysis confirms previous research observations that suggest a strong dependence on the finite element mesh for the smeared crack model [1, 5, 11, 12].

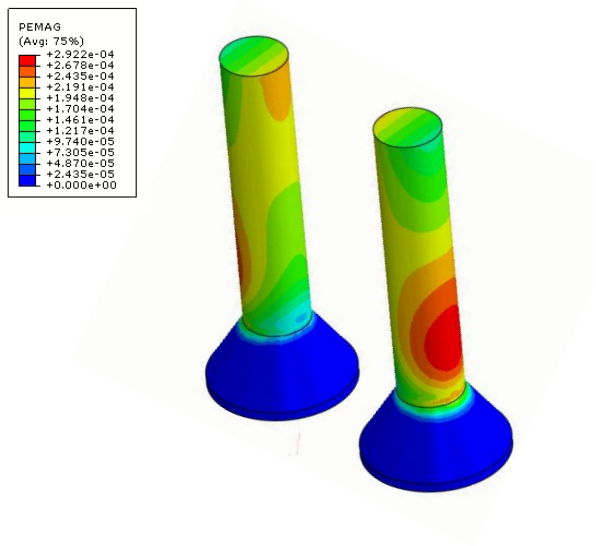

a. 3D Perspective.

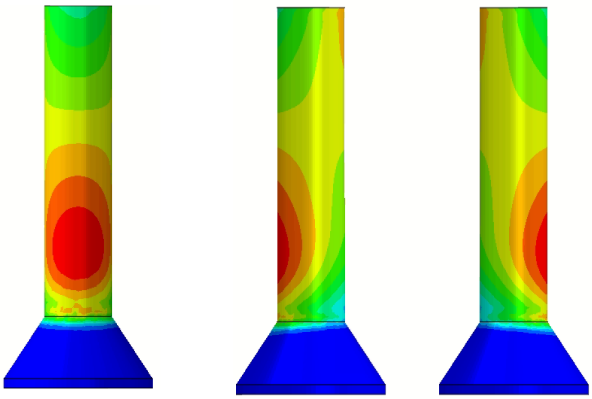

b. 2D right. c. 2D front.

Figure 15: Crack pattern in the local model for full-service load.

Concerning the principal stresses observed for the local model (Figure 16), stresses of 1.367 MPa were observed. This result is significantly higher than the 0.2 MPa obtained for the global model (Figure 12). In general terms, there are numerous advantages to using the submodeling technique due to the patterns of results explained in this paper.

Finally, part of the dispersion found in the results can be mitigated by using mesh objectivity studies. However, this strategy may increase the model processing time.

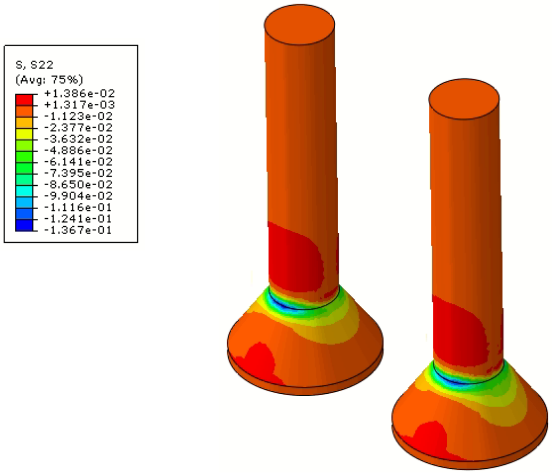

Figure 16: Principal stresses for full-service load in the local model (kN/cm²).

12 CONCLUSIONS

From the results shown in this paper, the main points below can be concluded:

- The submodeling technique can be applied to concrete structures in conjunction with smeared cracking models.
- Advantages were verified for identifying results in the local model, among which stand out the superior values of principal stresses, deformations in cracks, and prediction of cracking loads when compared with the responses of the global model.
- It is suggested to use a submodeling approach at the same hierarchy level described in this work (solid-to-solid) to avoid compatibility problems and uncertainties about the computational results obtained.
- Using conventional modeling techniques can cause inaccurate results, especially those related to principal stresses and deformations in cracks.
- The submodeling technique proved advantageous for analyzing the reinforced concrete railway bridge section presented in this paper, mainly

due to the presence of geometric discontinuities in the foundations.

REFERENCES

[1] Rots, J.G. and Blaauwendraad, J., 1989. Crack models for concrete: discrete or smeared? Fixed, multi-directional or rotating? *Heron* **34**: 5-59.

[2] Yang, Z. and Chen, J., 2004. Fully automatic modelling of cohesive discrete crack propagation in concrete beams using local arc-length methods. *Int. J. Solids Struct.* **41**:801-826.

[3] Cervera, M. and Chiument, M., 2006. Smeared crack approach: back to the original track. *Int. J. Numer. Anal. Methods Geomech.* **30**: 1173-1199.

[4] Oliver-Leblond, C., Delaplace, A. and Ragueneau, F., 2015. Modelling of three-dimensional crack patterns in deep reinforced concrete structures. *Eng. Struc.* **83**: 176-186.

[5] Jirásek, M. and Zimmermann, T., 1998. Rotating crack model with transition to scalar damage. *J. Eng. Mech.* **124**: 277-284.

[6] Evangelista Jr., F., Alves, G.S., Moreira, J.F.A. and Paiva, G.O.F., 2020. A global–local strategy with the generalized finite element framework for continuum damage models. *Comput. Methods Appl. Mech. Engrg.* **363**: 1-19.

[7] Liu, Z., Correia, J., Carvalho, H., Mourão, A., Jesus, A., Calçada, R. and Berto, F., 2020. Global-local fatigue assessment of an ancient riveted metallic bridge based on submodelling of the critical detail. *Fatigue Fract. Eng. Mater. Struct.* **42**: 546-560.

[8] ABAQUS, 2014. Version 6.14 User's Manual. Dassault Systèmes.

[9] Associação Brasileira de Normas Técnicas (ABNT), 2014. *Projeto de estruturas de concreto - procedimento. NBR 6118*. ABNT.

[10] Kupfer, H., Hilsdorf, H.K. and Rusch, H., 1969. Behavior of concrete in under biaxial stresses. *ACI Struct. J.* **66**: 656-666.

[11] Jirásek, M. and Zimmermann, T., 1998. Rotating crack model with transition to scalar damage. *J. Eng. Mech. ASCE* **124**: 277-284.

[12] Petrangeli, M. and Ozbolt, J., 1996. Smeared crack approaches – material modeling. *J. Eng. Mech.* **122**: 545-554.